

Article

Process Parameters Optimization of Gallic Acid Removal from Water by MIEX Resin Based on Response Surface Methodology

Qiang Zhou ¹, Lei Ding ^{1,2,*}, Yunhua Zhu ^{1,2}, Meiyong Zhong ^{1,2} and Chuchu Yang ¹

¹ School of Civil Engineering and Architecture, Anhui University of Technology, 59 Hudong Road, Maanshan 243002, China; zhouqiang_1995@163.com (Q.Z.); zhuchem01@163.com (Y.Z.); zhongmy@ahut.edu.cn (M.Z.); yccchuchu@163.com (C.Y.)

² Engineering Research Center of Biomembrane Water Purification and Utilization Technology, Ministry of Education, 59 Hudong Road, Maanshan 243002, China

* Correspondence: dllyan@ahut.edu.cn

Received: 26 November 2019; Accepted: 27 January 2020; Published: 27 February 2020



Abstract: In this work, the response surface methodology was used to optimize the process parameters of gallic acid adsorption on magnetic ion exchange (MIEX) resin. Based on Box-Behnken Design, a quadratic polynomial model equation including solution pH, gallic acid concentration, MIEX resin dosage and adsorption time was established. The reliability of the established regression equation was tested by variance analysis. Based on the regression equation, the technical parameters for gallic acid adsorption on MIEX resin were optimized and the effects of interaction between variables on the removal of gallic acid were analyzed. The results showed that the established regression equation was reliable and could effectively predict the removal of gallic acid. The optimal technical parameters were determined to be a pH of 9.17, a gallic acid concentration of 8.07 mg/L, a resin dosage of 0.98 mL/L and an adsorption time of 46.43 min. The removal efficiency of gallic acid was 97.93% under the optimal parameters. The interaction between pH and adsorption time had the most significant effect on the removal of gallic acid. The results of this study demonstrated that MIEX resin can remove gallic acid efficiently and relatively quickly under the condition of optimal technical parameters.

Keywords: MIEX resin; gallic acid; process parameters optimization; adsorption; response surface methodology

1. Introduction

Natural organic matter (NOM) widely exists in surface water and groundwater sources due to the breakdown of biomass [1]. Gallic acid (GA) is a typical fraction of NOM. In addition, GA has been widely used in prints and dyes, medicine, food and the metallurgical industry [2–4]. Unfortunately, a great deal of wastewater containing GA discharges into water bodies. Moreover, it is difficult to remove GA by the traditional drinking water treatment processes due to its water solubility and small molecular weight [5,6]. It has been demonstrated that excess GA in water bodies causes the unpleasant color and odor of drinking water, and the formation of carcinogenic disinfection by-products (DBPs), such as trichloroethanes and chloroacetic acids, during the chlorination process [7–9]. Therefore, it is necessary to remove GA from raw water to guarantee the safety of drinking water.

Various techniques have been used to remove GA from waters. Electrochemistry is a good way, but the power consumption is high and the electricity utilization rate is low. Fenton processes, including the electrochemical Fenton treatment, the photo-Fenton treatment [10,11], have been employed to remove GA, but there may be secondary contamination of the intermediates. Biosorption techniques have been used to adsorb GA, but even low concentrations of GA may inhibit microbial growth [5].

Adsorption technology using different adsorbents has aroused concerns due to its convenient operation, high removal efficiency and adsorbent reusability. Many adsorbents have been utilized for the removal of GA, such as clay minerals [12,13] and activated carbon [14,15]. Activated carbon can remove GA from aqueous solution effectively. The regeneration of activated carbon should be done in order to recover its adsorption ability. Heat treatment is often used to regenerate saturated activated carbon, but plenty of energy is required.

Li et al. [16] found that temperature has the most important influence on activated carbon regeneration. In recent years, some resins [17,18], such as ZDX-1, WJN-09, XC-1, HP-2MG, XAD-7, XAD-761, XAD-4 and XAD-16, have been used for the removal of GA from waters due to its easy regeneration compared with activated carbon. However, it has a relatively slow adsorption kinetic process for conventional resin due to the large size (>0.4 mm) of resin particles. A magnetic ion exchange (MIEX) resin, developed by Orica Watercare, is a macro-porous anion resin with two properties: smaller particle size (average 0.15 mm) and magnetism [19]. MIEX resin is distinguishable by its great specific surface area, which is 2–5 fold larger than traditional resins. In addition, MIEX resin can be efficiently separated from water due to its magnetism. The magnetism of MIEX resin is caused by the iron oxide ($\gamma\text{-Fe}_2\text{O}_3$) incorporated into its polyacrylic matrix. Owing to its small size, MIEX resin can be used in a slurry form and mixed well with adsorbate by mechanical stirring at a speed of 100–150 rpm. With a decrease in the stirring speed, resin particles can rapidly aggregate and settle at the bottom of the reactor. MIEX resin was mainly designed for the removal of dissolved organic matter from raw water and wastewater, and has been used to remove DOC [20,21], UV_{254} [22,23], MIB and geosmin [24], estrone [25], pesticide [26], 2,4-D [27], bisphenol A [28] and inorganic ion [29]. As an anion exchange resin, MIEX resin can potentially remove GA from raw water. However, to the authors' knowledge, the adsorption of GA by MIEX resin has not been reported yet. Particularly, the process parameters for GA removal by MIEX resin have not been optimized. These parameters are essential for MIEX resin to effectively remove GA from raw water.

Response Surface Methodology (RSM), as a scientific research method, combines mathematical and statistical technologies. The authors propose this method to evaluate the factors affecting complex processes and their interactions [30]. Compared with the traditional analytical method, RSM can be applied to optimize process parameters in multivariate conditions and to reduce the number of experiments. The steps of the RSM include designing experiments, establishing mathematical models and optimizing experiments. RSM has been widely used to optimize the process parameters for the removal of heavy metals, dyes and natural organic compounds [31–33].

Therefore, the main purpose of this study was to optimize the factors influencing the removal of GA by MIEX resin. Based on the RSM experiments, a quadratic polynomial equation was established. The reliability of the model equation was analyzed. The effects of interaction between variables on the removal of GA were investigated. Finally, the process parameters were optimized. In practice, the optimal MIEX resin dosage, adsorption time and pH of raw water can be obtained by the established regression equation at a certain concentration of GA in raw water.

2. Materials and Methods

2.1. Materials and Reagents

MIEX resin, as an adsorbent, was bought from Beijing Orica Technology & Equipment Co., Ltd., Beijing, China. GA (purity 99%), and other agents were purchased from Sinopharm Chemical Reagent Co., Ltd., Shanghai, China, which were at least of analytical grade.

The standard stock solution of GA (1000 mg/L) was obtained by dissolving 0.5051 g GA powder into 500 mL ultrapure water. Test solutions were prepared by diluting the standard stock solution when necessary. The molecular weight of GA is 170.11954 g/mol and the molecular structure of GA contains three adjacent phenolic hydroxyl groups and a carboxyl group.

2.2. Adsorption Tests

Batch experiments regarding GA adsorption by MIEX resin were conducted on a program-controlled jar test apparatus (ZR4-6, Shenzhen Zhong-run Water Industry Technology and Development Co., Ltd., Shenzhen, China) at room temperature (293 K) with a stirring speed of 150 rpm. A certain amount of MIEX resin was mixed into 500 mL GA solution. After adsorption, the slurry was filtered by 0.22 μm Millipore membranes. The GA concentration in filtrate was determined by an ultraviolet spectrophotometer (UV9600 UV spectrophotometer, Beijing Ruili Analytical Instrument Co., Ltd., Beijing, China) [34]. All of the experiments were performed in triplicate and the average values were calculated. The removal efficiency of GA by MIEX resin was then calculated by Equation (1).

$$E(\%) = (C_0 - C_t) / C_0 \times 100 \quad (1)$$

where C_0 is the initial concentration of GA (mg/L); C_t is the concentration of GA (mg/L) in solution at adsorption time t .

2.3. Analytical Methods

The concentration of GA was determined by a UV9600 ultraviolet spectrophotometer. The maximum absorption peak for GA was found at a wavelength of 264 nm, therefore the measurement wavelength of GA was set at this level. The pH of the GA solution was determined using a pH meter (pHS-3C model, Leici, Shanghai, China).

In this study, the experimental design of response surface methodology, analysis of variance, three-dimensional response surface plot and two-dimensional contour plot were conducted by Design-Expert 8.0 (State-Ease Inc., Minneapolis, MN, USA).

2.4. Experimental Design of Response Surface Methodology

According to the Box-Behnken Design (BBD) model, the experiments of RSM were designed by Design-Expert 8.0 software (State-Ease Inc., Minneapolis, MN, USA). In our pre-experiments, we found that temperature had less effect on the adsorption of GA on MIEX resin, and the effect of agitation speed could be neglected when the speed exceeds 150 rpm. Therefore, four parameters including solution pH, GA concentration, MIEX resin dosage and adsorption time were selected as independent variables and were signed as X_1 , X_2 , X_3 and X_4 , respectively. For each variable, three different levels of codes were given as -1 , 0 and $+1$, representing low, medium and high, respectively. Table 1 lists the levels and ranges of selected variables in this study. Based on the BBD model, 27 tests of GA adsorption on MIEX resin were designed. In accordance with Equation (2) [35], all variables for each test were given with different coded values. These coded values and the actual variables' values were given in Table 2.

$$x_i = (X_i - X_0) / \Delta X_i \quad (2)$$

where X_i is the actual experimental value of the i th independent variable, X_0 is the actual experimental value of the i th independent variable at the center point, ΔX_i is the independent variable step size and x_i is the encoded value of the i th independent variable.

Table 1. The selected factors and levels of Response Surface Methodology (RSM) experiments.

Factor	Code	Level		
		-1	0	1
Solution pH	X_1	3.0	7.0	11.0
GA concentration (mg/L)	X_2	5	10	15
MIEX resin dosage (mL/L)	X_3	0.2	0.6	1
Adsorption time/min	X_4	20	40	60

Table 2. RSM experimental design and the results.

Run	Actual Value				Coded Value				Removal Efficiency, E (%)	
	X ₁	X ₂	X ₃	X ₄	X ₁	X ₂	X ₃	X ₄	Experimental	Predicted
1	3.0	15	0.6	40	-1	1	0	0	6.27 ^{+2.76} _{-1.33}	9.57
2	11.0	10	1.0	40	1	0	1	0	83.17 ^{+4.61} _{-1.59}	89.42
3	3.0	10	0.6	60	-1	0	0	1	4.33 ^{+1.65} _{-0.86}	10.48
4	7.0	10	0.6	40	0	0	0	0	73.04 ^{+2.28} _{-2.79}	73.74
5	3.0	5	0.6	40	-1	-1	0	0	5.00 ^{+0.46} _{-0.28}	7.29
6	3.0	10	0.2	40	-1	0	-1	0	0.40 ^{+0.07} _{-0.03}	0.65
7	11.0	10	0.2	40	1	0	-1	0	51.91 ^{+1.48} _{-3.47}	45.47
8	7.0	5	0.6	20	0	-1	0	-1	49.66 ^{+3.87} _{-2.78}	53.43
9	7.0	10	1.0	60	0	0	1	1	93.99 ^{+0.37} _{-1.12}	93.56
10	7.0	5	1.0	40	0	-1	1	0	85.46 ^{+1.29} _{-3.81}	81.52
11	7.0	15	1.0	40	0	1	1	0	89.37 ^{+0.77} _{-3.82}	85.29
12	7.0	5	0.6	60	0	-1	0	1	84.60 ^{+2.23} _{-1.15}	77.90
13	7.0	10	0.6	40	0	0	0	0	76.42 ^{+1.21} _{-2.65}	73.74
14	3.0	10	0.6	20	-1	0	0	-1	5.39 ^{+0.67} _{-1.11}	1.07
15	7.0	15	0.6	60	0	1	0	1	87.12 ^{+1.59} _{-3.46}	79.56
16	7.0	5	0.2	40	0	-1	-1	0	43.11 ^{+2.13} _{-1.48}	47.32
17	11.0	10	0.6	20	1	0	0	-1	55.08 ^{+1.64} _{-2.81}	49.07
18	7.0	10	1.0	20	0	0	1	-1	68.36 ^{+0.11} _{-0.45}	67.93
19	11.0	5	0.6	40	1	-1	0	0	70.31 ^{+0.11} _{-0.34}	70.68
20	3.0	10	1.0	40	-1	0	1	0	16.08 ^{+1.43} _{-0.89}	18.71
21	7.0	15	0.6	20	0	1	0	-1	52.50 ^{+2.56} _{-1.44}	55.39
22	7.0	10	0.2	60	0	0	-1	1	52.00 ^{+1.42} _{-1.87}	56.10
23	7.0	10	0.6	40	0	0	0	0	71.75 ^{+1.54} _{-2.31}	73.74
24	11.0	10	0.6	60	1	0	0	1	83.86 ^{+3.28} _{-1.41}	88.31
25	11.0	15	0.6	40	1	1	0	0	70.63 ^{+1.32} _{-1.69}	72.01
26	7.0	10	0.2	20	0	0	-1	-1	28.98 ^{+1.29} _{-1.33}	33.08
27	7.0	15	0.2	40	0	1	-1	0	43.10 ^{+2.06} _{-1.91}	47.17

The superscript and subscript represent the deviation of the experimental values. For example, 6.27-average of three determinations; +2.76-positive deviation; -1.33-negative deviation. (Run 1).

The removal percent of GA by MIEX resin was denoted as the response value E (%). A quadratic polynomial regression model (given by Equation (3)) [36] was established to fit the experimental data.

$$E(\%) = h_0 + \sum h_i x_i + \sum h_{ii} x_i^2 + \sum h_{ij} x_i x_j + \varepsilon \quad (3)$$

where h_0 is a constant coefficient, h_i is the linear regression coefficient of the i th input variable, h_{ii} is the quadratic regression coefficient of the i th input variable, h_{ij} is the interactive effect regression coefficient between the input variables, x_i and x_j are the input variables x_j and x_j , and ε is the random error.

3. Results

3.1. Fitting of Regression Model Equation

Twenty-seven experiments of GA adsorption on MIEX resin were conducted. The removal efficiencies of GA, calculated using Equation (1), are shown in Table 2. Equation (3) was used to fit the experimental data, and the regression model equation including solution pH, GA concentration, MIEX resin dosage and adsorption time, was obtained by Equation (4). Based on Equation (4), the predicted removal efficiency of GA was calculated and summarized in Table 2. The predicted responses vary from 0.65% to 93.56%, indicating that GA removal is related to the parameters selected in this study [37].

$$E(\%) = 73.74 + 31.46x_1 + 0.91x_2 + 18.08x_3 + 12.16x_4 - 0.23x_1x_2 + 3.90x_1x_3 + 7.46x_1x_4 + 0.98x_2x_3 - 0.08x_2x_4 + 0.65x_3x_4 - 31.59x_1^2 - 2.26x_2^2 - 6.16x_3^2 + x_4^2 \quad (4)$$

3.2. Reliability Analysis of the Regression Model Equation

The coefficient of determination (R^2) and the standard deviation (SD) of the regression model equation can be used to evaluate the reliability of the regression equation. The R^2 of regression equation is 0.98, showing that the experimental and predicted values in GA removal are close. Additionally, the SD of 6.81 further demonstrates that the regression model equation has a good degree of fitting. The R^2 value of 0.98 means that the regression model equation can explain the change of 98% of response values. The “Predicted R^2 ” of 0.87 is reasonably consistent with the “Adjusted R^2 ” of 0.95, showing that the predicted value has a significant correlation with the actual value [38]. In addition, the high precision of the quadratic polynomial regression equation was proved by a relatively small coefficient of variation (CV = 12.66%) [39]. A high “Adequate Precision” value of 20.35, much higher than 4, is desirable for the regression equation, indicating an adequate signal [40]. These results imply that the obtained regression model equation (Equation (4)) in this study is statistically valid for describing the removal of GA by MIEX resin under the experimental conditions.

Moreover, analysis of variance (ANOVA) can be applied to test the reliability of the quadratic polynomial regression equation [41], as demonstrated in Table 3. In ANOVA, the f -value and p -value determine the significance of the regression model equation or the coefficient terms of the model. The larger f -value and smaller p -value (<0.05) were considered to determine whether the regression model is statistically significant [42,43]. The f -value, shown in Table 3, is 36.57, and the p -value is less than 0.0001, indicating that the regression model equation in this study is extremely significant and highly reliable. The p -value of 0.1002 (>0.05) for “Lack of fit” means that the lack of fit is not significant and the adverse influence on the accuracy of the model equation can be neglected.

Table 3. Variance and significance analysis.

Source	Sum of Squares	Degree of Freedom	Mean Square	F	Prob > F
Model	23,701.35	14	1692.95	36.57	<0.0001
X_1 -pH	11,873.99	1	11,873.99	256.47	<0.0001
X_2 -GA concentration	9.84	1	9.84	0.21	0.5392
X_3 -Resin dosage	3921.36	1	3921.36	84.70	<0.0001
X_4 -Adsorption time	1774.60	1	1774.60	38.33	<0.0001
X_1X_2	0.22	1	0.22	0.01	0.9456
X_1X_3	60.70	1	60.70	1.31	0.2745
X_1X_4	222.61	1	222.61	4.81	0.0488
X_2X_3	3.85	1	3.85	0.08	0.7779
X_2X_4	0.03	1	0.03	0.00	0.9823
X_3X_4	1.70	1	1.70	0.04	0.8514
X_1^2	5323.96	1	5323.96	114.99	<0.0001
X_2^2	27.14	1	27.14	0.59	0.4586
X_3^2	202.25	1	202.25	4.37	0.0586
X_4^2	128.75	1	128.75	2.78	0.1213
Residual	555.57	12	46.30		
Lack of fit	543.97	10	54.40	9.38	0.1002
Pure error	11.60	2	5.80		
Cor total	24,256.92	26			

The internally studentized residuals and normal probability plot of GA removal by MIEX resin are shown in Figure 1. In general, the residuals were calculated from the difference between the experimental value and the predicted value. The normality analysis of the residuals of the quadratic polynomial model was used to determine whether the model satisfies the assumptions of ANOVA [43,44]. Figure 1 shows that the experimental results are distributed normally. Accordingly, the established model equation in this study is reliable and can be used to predict the adsorption of GA on MIEX resin in the experimental range.

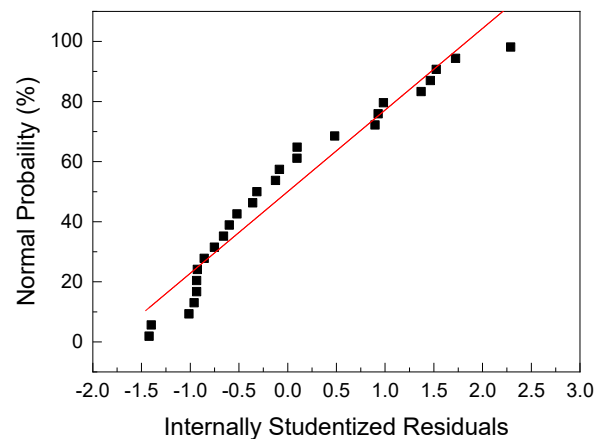


Figure 1. The normal probability plot of the internally studentized residuals for Gallic acid (GA) adsorption.

3.3. Significant Degree of Independent Variables on GA Removal

In improving adsorption conditions, it is helpful to understand the degree of influence of each independent variable on GA adsorption by MIEX resin. The main effect plots of various independent variables are plotted in Figure 2 and used to analyze the degree of influence of each independent variable. For one factor, the more the mean removal efficiency changes with a change in the level from low to high, the greater the influence of the factor on GA removal [42,45]. It can be seen from Figure 2a–d that among the four parameters, increasing the pH from 3.0 to 11.0 caused the largest change in the mean removal efficiency, indicating that solution pH (X_1) is the most important parameter affecting GA removal. The order of significance of the independent variables affecting GA removal is as follows: solution pH > MIEX resin dosage > adsorption time > GA concentration. This is consistent with the ANOVA results given in Table 3, according to the sum of squares and P values of four independent variables [46].

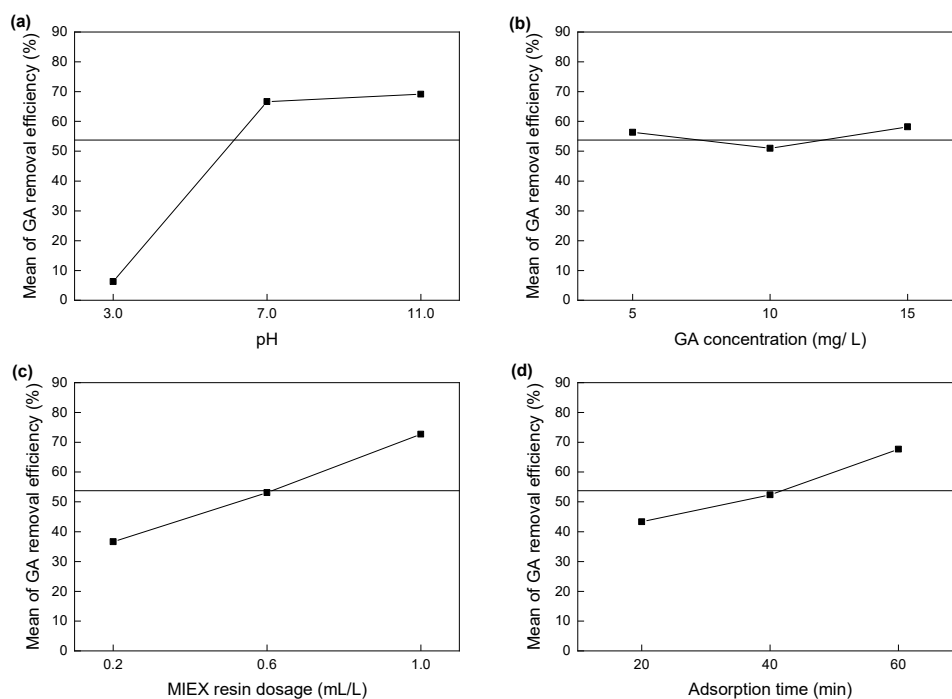


Figure 2. Main effect plots of four parameters for GA removal efficiency (%). (a) solution pH; (b) GA concentration; (c) MIEX resin dosage; (d) adsorption time.

3.4. Influences of Interactions between Variables on GA Removal

The combined interaction between variables (parameters) may affect the GA adsorption by MIEX resin. Understanding the interaction between variables is helpful to achieve the largest removal efficiency and the optimal process conditions to remove the maximum volume of GA.

It can be seen from Table 3 that for all the interactive terms in the model equation, the p -values of X_1X_3 and X_1X_4 are 0.2745 and 0.0488, respectively. This shows that the effects of the interaction between pH and resin dosage, as well as pH and adsorption time on the removal of GA, are statistically significant. The effects of the interaction between other variables, on the other hand, are not significant. Therefore, pH, resin dosage and adsorption time are selected for discussion on the combined effects of interactions between these factors on the removal of GA. Based on the established regression model, the influences of interactions between these variables on responses can be visualized by a three-dimensional response surface and two-dimensional contour plots [47]. Figures 3 and 4 depict, by Design-Expert 8.0 software, the 3D response surface and contour plots of the interactions between pH and resin dosage, and pH and adsorption time, respectively.

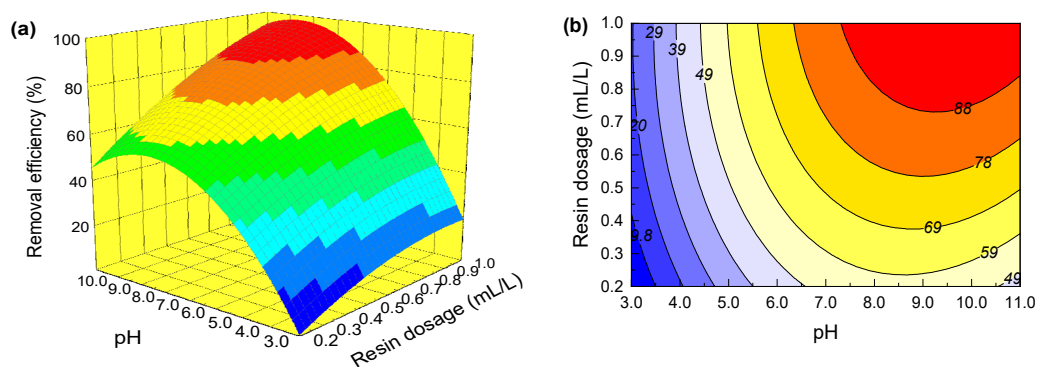


Figure 3. (a) Response surface showing the combined effect of pH and MIEX resin dosage on GA removal; (b) contour plots showing the combined effect of pH and MIEX resin dosage on GA removal.

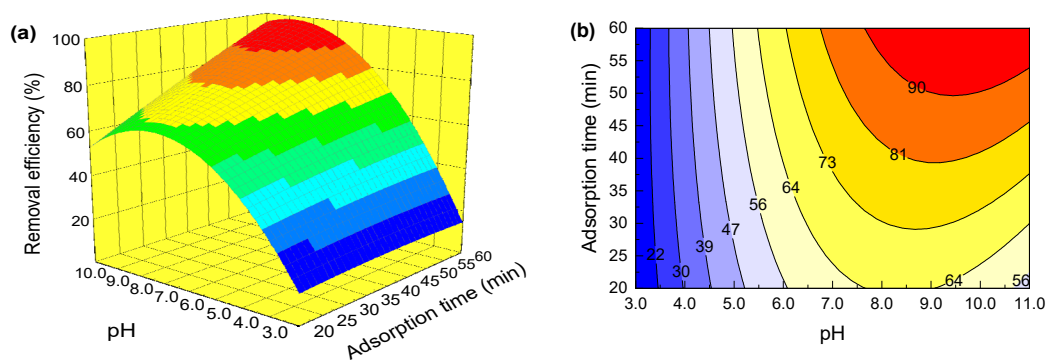


Figure 4. (a) Response surface showing the combined effect of pH and adsorption time on GA removal; (b) contour plots showing the combined effect of pH and adsorption time on GA removal.

Figure 3 gives the combined effects of the interaction between solution pH and MIEX resin dosage on GA removal under the condition of 10 mg GA/L and a 40 min adsorption. It can be seen from Figure 3a that the removal efficiency of GA increases with an increase of solution pH and resin dosage. The high pH is helpful for the removal of GA, a fact that could be explained by the formation of anion-led GA exchange with chloride occurring on the active sites of MIEX resin [48]. The more MIEX resin particles supply, the more available active sites, thus promoting GA removal [5]. In contrast, solution pH contributes more than resin dosage to GA removal. In respect of the contour plots, an elliptical or saddle shape implies that the interaction between variables is significant [49]. From this perspective, it can be seen obviously from Figure 3b that the effect of interaction between solution

pH and MIEX resin dosage is significant. Figure 3b further shows that the optimal GA removal rate (97.55%) occurs at a solution pH of 9.6 and a resin dosage of 1.0 mL/L.

The response surface and contour plots are depicted in Figure 4 to reflect the effect of the interaction between solution pH and adsorption time on GA removal under the constant conditions of a GA concentration of 10 mg/L and an adsorption time of 40 min. It can be seen from Figure 4 that the interaction between solution pH and adsorption time has a significant effect on the removal of GA. The efficiency of GA removal increases rapidly with an increase in pH from 3.0 to 7.0, then decreases slightly with an increase in pH to 11.0. Additionally, the effect of solution pH is much more significant than that of adsorption time. The removal rate of GA attains the maximum of 97.91% at a pH of 9.8 and an adsorption time of 60 min.

3.5. Optimal Adsorption Parameters and Confirmation Experiments

The main goal of this work was to find out the optimal process parameters for the adsorption of GA on MIEX resin using the established model equations. Design-Expert 8.0 software was used to establish the regression equation (Equation (4)) and the optimal process parameters, and the predicted removal rate of GA by MIEX resin were obtained. The results are given in Table 4. The optimal conditions are as follows: a pH of 9.17, a GA concentration of 8.07 mg/L, a resin dosage of 0.98 mL/L, and an adsorption time of 46.43 min. Under these optimal conditions, the maximum removal efficiency of GA was 98.99%. According to the optimal conditions above, three sets of parallel tests were carried out and the average removal efficiency of GA reached 97.93%, a figure very close to the predicted value of 98.99%. This shows that the established model equation in this study is applicable to the prediction of GA adsorption by MIEX resin.

Table 4. Optimal process conditions for GA removal by Magnetic Ion Exchange (MIEX) resin.

pH	GA Concentration (mg/L)	Resin Dosage (mL/L)	Adsorption Time (min)	Removal Efficiency of GA, E (%)	
				Predicted	Experimental
9.17	8.07	0.98	46.43	98.99	97.93 ^{+1.21} _{-0.64}

4. Conclusions

The authors proposed a quadratic polynomial model equation including four factors—solution pH, gallic acid concentration, MIEX resin dosage and adsorption time—to predict the adsorption of GA by MIEX resin and to optimize the process parameters. The equation was proved to have good reliability and to be able to effectively predict whether GA had been effectively removed. Solution pH was the most important parameter affecting GA removal. The order of significance of independent variables affecting GA removal was solution pH > MIEX resin dosage > adsorption time > GA concentration. The interaction between pH and adsorption time, as well as between pH and MIEX resin dosage had significant effects on the GA removal. The optimal process parameters for GA removal were a pH of 9.17, a GA concentration of 8.07 mg/L, a resin dosage of 0.98 mL/L and an adsorption time of 46.43 min. The removal efficiency of GA under these conditions was 97.93%. MIEX resin can remove GA efficiently and relatively quickly from aqueous solution. In future research, the removal of GA, the costs in a continuous operation process and the optimal process parameters for real raw water need to be studied.

Author Contributions: Investigation, Y.Z., Q.Z. and M.Z.; Writing—Original Draft Preparation, Q.Z. and C.Y.; Writing—Review & Editing, Q.Z. and L.D.; Supervision, L.D. All authors have read and agreed to the published version of the manuscript.

Funding: This research was funded by the National Natural Science Foundation of China (Grant No. 51308001), the Project of Cultivating Top Talents for the Universities in Anhui Province (Grant No. gxyqZD2017036), and Scientific and the Innovation and Entrepreneurship Training Program of China for Undergraduate (Grant No. 2018110360077).

Conflicts of Interest: The authors declare no conflict of interest.

References

1. Awad, J.; van Leeuwen, J.; Chow, C.; Drikas, M.; Smernik, R.J.; Chittleborough, D.J.; Bestland, E. Characterization of dissolved organic matter for prediction of trihalomethane formation potential in surface and sub-surface waters. *J. Hazard. Mater.* **2016**, *308*, 430–439. [[CrossRef](#)] [[PubMed](#)]
2. Shahamirifard, S.A.; Ghaedi, M.; Razmi, Z.; Hajati, S. A simple ultrasensitive electrochemical sensor for simultaneous determination of gallic acid and uric acid in human urine and fruit juices based on zirconia-choline chloride-gold nanoparticles-modified carbon paste electrode. *Biosens. Bioelectron.* **2018**, *114*, 30–36. [[CrossRef](#)] [[PubMed](#)]
3. Bahrani, S.; Ghaedi, M.; Daneshfar, A. Fabrication of size controlled nanocomposite based on zirconium alkoxide for enrichment of gallic acid in biological and herbal tea samples. *J. Chromatogr. B* **2018**, *1087–1088*, 14–22. [[CrossRef](#)] [[PubMed](#)]
4. Vilian, A.T.E.; Song, J.Y.; Lee, Y.S.; Hwang, S.-K.; Kim, H.J.; Jun, Y.S.; Huh, Y.S.; Han, Y.K. Salt-templated three-dimensional porous carbon for electrochemical determination of gallic acid. *Biosens. Bioelectron.* **2018**, *117*, 597–604. [[CrossRef](#)] [[PubMed](#)]
5. Zhang, Z.; Pang, Q.; Li, M.; Zheng, H.; Chen, H.; Chen, K. Optimization of the condition for adsorption of gallic acid by *Aspergillus oryzae mycelia* using Box-Behnken design. *Environ. Sci. Pollut. Res. Int.* **2015**, *22*, 1085–1094. [[CrossRef](#)]
6. Lu, L.L.; Lu, X.Y. Solubilities of gallic acid and its esters in water. *J. Chem. Eng. Data* **2007**, *52*, 37–39. [[CrossRef](#)]
7. Fiuza, S.M.; Gomes, C.; Teixeira, L.J.; Girão da Cruz, M.T.; Cordeiro, M.N.D.S.; Milhazes, N.; Borges, F.; Marques, M.P.M. Phenolic acid derivatives with potential anticancer properties—A structure-activity relationship study. Part 1: Methyl, propyl and octyl esters of caffeic and gallic acids. *Bioorg. Med. Chem.* **2004**, *12*, 3581–3589. [[CrossRef](#)]
8. Wu, Y.; Zhou, K.; Dong, S.; Yu, W.; Zhang, H. Recovery of gallic acid from gallic acid processing wastewater. *Environ. Technol.* **2015**, *36*, 661–666. [[CrossRef](#)]
9. Víctor-Ortega, M.D.; Airado-Rodríguez, D. Revalorization of agro-industrial effluents based on gallic acid recovery through a novel anionic resin. *Process Saf. Environ. Prot.* **2018**, *115*, 17–26. [[CrossRef](#)]
10. Boye, B.; Brillas, E.; Buso, A.; Farnia, G.; Flox, C.; Giomo, M.; Sandonà, G. Electrochemical removal of gallic acid from aqueous solutions. *Electrochim. Acta* **2007**, *52*, 256–262. [[CrossRef](#)]
11. Benitez, F.J.; Real, F.J.; Acero, J.L.; Leal, A.I.; Garcia, C. Gallic acid degradation in aqueous solutions by UV/H₂O₂ treatment, Fenton's reagent and the photo-Fenton system. *J. Hazard. Mater.* **2005**, *126*, 31–39. [[CrossRef](#)] [[PubMed](#)]
12. Rabiei, M.; Sabahi, H.; Rezayan, A.H. Gallic acid-loaded montmorillonite nanostructure as a new controlled release system. *Appl. Clay Sci.* **2016**, *119*, 236–242. [[CrossRef](#)]
13. Ahmat, A.M.; Thiebault, T.; Guégan, R. Phenolic acids interactions with clay minerals: A spotlight on the adsorption mechanisms of gallic acid onto montmorillonite. *Appl. Clay Sci.* **2019**, *180*, 105188. [[CrossRef](#)]
14. Mammari, A.C.; Mouni, L.; Bollinger, J.C.; Belkhir, L.; Bouzaza, A.; Assadi, A.A.; Belkacemi, H. Modeling and optimization of process parameters in elucidating the adsorption mechanism of gallic acid on activated carbon prepared from date stones. *Sep. Sci. Technol.* **2019**, in press. [[CrossRef](#)]
15. Cagnon, B.; Chedeville, O.; Cherrier, J.F.; Caqueret, V.; Porte, C. Evolution of adsorption kinetics and isotherms of gallic acid on an activated carbon oxidized by ozone: Comparison to the raw material. *J. Taiwan Inst. Chem. Eng.* **2011**, *42*, 996–1003. [[CrossRef](#)]
16. Li, Y.; Lin, Y.; Wang, B.; Ding, S.; Qi, F.; Zhu, T. Carbon consumption of activated coke in the thermal regeneration process for flue gas desulfurization and denitrification. *J. Clean. Prod.* **2019**, *228*, 1391–1400. [[CrossRef](#)]
17. Wang, J.N.; Li, A.M.; Xu, L.; Zhou, Y. Adsorption of tannic and gallic acids on a new polymeric adsorbent and the effect of Cu(II) on their removal. *J. Hazard. Mater.* **2009**, *169*, 794–800. [[CrossRef](#)]
18. Kaleh, Z.; Geißen, S.U. Selective isolation of valuable biophenols from olive mill wastewater. *J. Environ. Chem. Eng.* **2016**, *4*, 373–384. [[CrossRef](#)]

19. Watson, K.; Farré, M.J.; Knight, N. Enhanced coagulation with powdered activated carbon or MIEX[®] secondary treatment: A comparison of disinfection by-product formation and precursor removal. *Water Res.* **2015**, *68*, 454–466. [[CrossRef](#)]
20. Rajca, M.; Bray, R.T.; Fitobor, K.; Golombek, K. Laser sizer granulometer as an useful tool for selection of appropriate membranes used in the MIEX[®] DOC-UF/MF hybrid process. *Arch. Metall. Mater.* **2018**, *63*, 1133–1140. [[CrossRef](#)]
21. Wolska, M. An evaluation of organic substance fraction removal during ion exchange with MIEX-DOC resin. *Environ. Sci. Pollut. Res. Int.* **2015**, *22*, 10360–10366. [[CrossRef](#)] [[PubMed](#)]
22. Jutaporn, P.; Laolertworakul, W.; Armstrong, M.D.; Coronell, O. Fluorescence spectroscopy for assessing trihalomethane precursors removal by MIEX resin. *Water Sci. Technol.* **2019**, *79*, 820–832. [[CrossRef](#)] [[PubMed](#)]
23. Gan, X.J.; Karanfil, T.; Bekaroglu, S.S.K.; Shan, J.H. The control of N-DBP and C-DBP precursors with MIEX[®]. *Water Res.* **2013**, *47*, 1344–1352. [[CrossRef](#)] [[PubMed](#)]
24. Drikas, M.; Dixon, M.; Morran, J. Removal of MIB and geosmin using granular activated carbon with and without MIEX pre-treatment. *Water Res.* **2009**, *43*, 5151–5159. [[CrossRef](#)]
25. Neale, P.A.; Mastrup, M.; Borgmann, T.; Schafer, A.I. Sorption of micropollutant estrone to a water treatment ion exchange resin. *J. Environ. Monit.* **2010**, *12*, 311–317. [[CrossRef](#)]
26. Liu, Z.Q.; Yan, X.M.; Drikas, M.; Zhou, D.N.; Wang, D.S.; Yang, M.; Qu, J.H. Removal of bentazone from micro-polluted water using MIEX resin: Kinetics, equilibrium, and mechanism. *J. Environ. Sci.* **2011**, *23*, 381–387. [[CrossRef](#)]
27. Ding, L.; Lu, X.; Deng, H.P.; Zhang, X.X. Adsorptive removal of 2,4-dichlorophenoxyacetic acid (2,4-D) from aqueous solutions using MIEX resin. *Ind. Eng. Chem. Res.* **2012**, *51*, 11226–11235. [[CrossRef](#)]
28. López-Ortiz, C.M.; Sentana-Gadea, I.; Varó-Galvañ, P.J.; Maestre-Pérez, S.E.; Prats-Rico, D. Effect of magnetic ion exchange (MIEX[®]) on removal of emerging organic contaminants. *Chemosphere* **2018**, *208*, 433–440. [[CrossRef](#)]
29. Rajca, M. The influence of selected factors on the removal of anionic contaminants from water by means of ion exchange MIEX[®] DOC process. *Arch. Environ. Prot.* **2012**, *38*, 115–121. [[CrossRef](#)]
30. Bezerra, M.A.; Santelli, R.E.; Oliveira, E.P.; Villar, L.S.; Escalera, L.A. Response surface methodology (RSM) as a tool for optimization in analytical chemistry. *Talanta* **2008**, *76*, 965–977. [[CrossRef](#)]
31. Karimifard, S.; Alavi Moghaddam, M.R. Application of response surface methodology in physicochemical removal of dyes from wastewater: A critical review. *Sci. Total Environ.* **2018**, *640–641*, 772–797. [[CrossRef](#)] [[PubMed](#)]
32. Yang, Y.; Ding, Q.; Yang, M.; Wang, Y.; Liu, N.; Zhang, X. Magnetic ion exchange resin for effective removal of perfluorooctanoate from water: Study of a response surface methodology and adsorption performances. *Environ. Sci. Pollut. Res. Int.* **2018**, *25*, 29267–29278. [[CrossRef](#)] [[PubMed](#)]
33. Uysal, S.; Cvetanovic, A.; Zengin, G.; Durovic, S.; Zekovic, Z.; Aktumsek, A. Effects of orange leaves extraction conditions on antioxidant and phenolic content: Optimization using response surface methodology. *Anal. Lett.* **2018**, *51*, 1505–1519. [[CrossRef](#)]
34. Dao, L.; Friedman, M. Chlorogenic acid content of fresh and processed potatoes determined by ultraviolet spectrophotometry. *J. Agric. Food. Chem.* **1992**, *40*, 2152–2156. [[CrossRef](#)]
35. Cho, I.-H.; Zoh, K.-D. Photocatalytic degradation of azo dye (Reactive Red 120) in TiO₂/UV system: Optimization and modeling using a response surface methodology (RSM) based on the central composite design. *Dyes Pigments* **2007**, *75*, 533–543. [[CrossRef](#)]
36. Hiew, B.Y.Z.; Lee, L.Y.; Lai, K.C.; Gan, S.; Thangalazhy-Gopakumar, S.; Pan, G.-T.; Yang, T.C.-K. Adsorptive decontamination of diclofenac by three-dimensional graphene-based adsorbent: Response surface methodology, adsorption equilibrium, kinetic and thermodynamic studies. *Environ. Res.* **2019**, *168*, 241–253. [[CrossRef](#)]
37. Zhang, X.X.; Lu, X.; Li, S.; Zhong, M.Y.; Shi, X.D.; Luo, G.; Ding, L. Investigation of 2,4-dichlorophenoxyacetic acid adsorption onto MIEX resin: Optimization using response surface methodology. *J. Taiwan Inst. Chem. Eng.* **2014**, *45*, 1835–1841. [[CrossRef](#)]
38. Ahmad, A.L.; Derek, C.J.C.; Zulkali, M.M.D. Optimization of thaumatin extraction by aqueous two-phase system (ATPS) using response surface methodology (RSM). *Sep. Purif. Technol.* **2008**, *62*, 702–708. [[CrossRef](#)]

39. Liu, J.; Yan, M.; Zhang, Y.K.; Du, K.F. Study of glutamate-modified cellulose beads for Cr(III) adsorption by response surface methodology. *Ind. Eng. Chem. Res.* **2011**, *50*, 10784–10791. [[CrossRef](#)]
40. Halder, G.; Dhawane, S.; Barai, P.K.; Das, A. Optimizing chromium (VI) adsorption onto superheated steam activated granular carbon through response surface methodology and artificial neural network. *Environ. Prog. Sustain. Energy* **2015**, *34*, 638–647. [[CrossRef](#)]
41. Anupam, K.; Dutta, S.; Bhattacharjee, C.; Datta, S. Adsorptive removal of chromium (VI) from aqueous solution over powdered activated carbon: Optimisation through response surface methodology. *Chem. Eng. J.* **2011**, *173*, 135–143. [[CrossRef](#)]
42. Bingol, D.; Tekin, N.; Alkan, M. Brilliant yellow dye adsorption onto sepiolite using a full factorial design. *Appl. Clay Sci.* **2010**, *50*, 315–321. [[CrossRef](#)]
43. Zhang, Z.; Zheng, H. Optimization for decolorization of azo dye acid green 20 by ultrasound and H₂O₂ using response surface methodology. *J. Hazard. Mater.* **2009**, *172*, 1388–1393. [[CrossRef](#)] [[PubMed](#)]
44. Zhang, K.; Cheung, W.H.; Valix, M. Roles of physical and chemical properties of activated carbon in the adsorption of lead ions. *Chemosphere* **2005**, *60*, 1129–1140. [[CrossRef](#)] [[PubMed](#)]
45. Palanikumar, K.; Davim, J.P. Assessment of some factors influencing tool wear on the machining of glass fibre-reinforced plastics by coated cemented carbide tools. *J. Mater. Process. Technol.* **2009**, *209*, 511–519. [[CrossRef](#)]
46. Zhang, B.; Han, X.; Gu, P.; Fang, S.; Bai, J. Response surface methodology approach for optimization of ciprofloxacin adsorption using activated carbon derived from the residue of desilicated rice husk. *J. Mol. Liq.* **2017**, *238*, 316–325. [[CrossRef](#)]
47. Bahrami, M.; Amiri, M.J.; Bagheri, F. Optimization of the lead removal from aqueous solution using two starch based adsorbents: Design of experiments using response surface methodology (RSM). *J. Environ. Chem. Eng.* **2019**, *7*, 102793. [[CrossRef](#)]
48. Song, X.R.; Chai, Z.H.; Zhu, Y.; Li, C.L.; Liang, X.Q. Preparation and characterization of magnetic chitosan-modified diatomite for the removal of gallic acid and caffeic acid from sugar solution. *Carbohydr. Polym.* **2019**, *219*, 316–327. [[CrossRef](#)]
49. Nourani, M.; Baghdadi, M.; Javan, M.; Bidhendi, G.N. Production of a biodegradable flocculant from cotton and evaluation of its performance in coagulation-flocculation of kaolin clay suspension: Optimization through response surface methodology (RSM). *J. Environ. Chem. Eng.* **2016**, *4*, 1996–2003. [[CrossRef](#)]



© 2020 by the authors. Licensee MDPI, Basel, Switzerland. This article is an open access article distributed under the terms and conditions of the Creative Commons Attribution (CC BY) license (<http://creativecommons.org/licenses/by/4.0/>).